The plant hormone ethylene restricts *Arabidopsis* growth via the epidermis

Irina Ivanova Vaseva[a,1], Enas Qudeimat[a,2], Thomas Potuschak[b], Yunlong Du[a,3], Pascal Genschik[b], Filip Vandenbussche[a], and Dominique Van Der Straeten[a,4]

[a]Laboratory of Functional Plant Biology, Department of Biology, Ghent University, B-9000 Ghent, Belgium; and [b]Institut de Biologie Moléculaire des Plantes du CNRS, IBMP-CNRS-Unité Propre de Recherche 2357, Strasbourg, France

Edited by James J. Giovannoni, USDA-ARS Robert W. Holley Center and Boyce Thompson Institute for Plant Research, Ithaca, NY, and approved March 19, 2018 (received for review October 9, 2017)

The gaseous hormone ethylene plays a key role in plant growth and development, and it is a major regulator of stress responses. It inhibits vegetative growth by restricting cell elongation, mainly through cross-talk with auxins. However, it remains unknown whether ethylene controls growth throughout all plant tissues or whether its signaling is confined to specific cell types. We employed a targeted expression approach to map the tissue site(s) of ethylene growth regulation. The ubiquitin E3 ligase complex containing Skp1, Cullin1, and the F-box protein EBF1 or EBF2 ($SCF^{EBF1/2}$) target the degradation of EIN3, the master transcription factor in ethylene signaling. We coupled EBF1 and EBF2 to a number of cell type-specific promoters. Using phenotypic assays for ethylene response and mutant complementation, we revealed that the epidermis is the main site of ethylene action controlling plant growth in both roots and shoots. Suppression of ethylene signaling in the epidermis of the constitutive ethylene signaling mutant *ctr1-1* was sufficient to rescue the mutant phenotype, pointing to the epidermis as a key cell type required for ethylene-mediated growth inhibition.

ethylene | auxin | EIN3 binding F-box factor EBF | root/shoot | *Arabidopsis*

The gaseous hormone ethylene modulates many aspects of plant biology ranging from vegetative development, control of ripening, abscission, senescence, and reproduction to stress responses (1, 2). In most plant tissues, ethylene causes growth reduction due to inhibition of cell expansion, in both roots and shoots (3, 4), acting by means of cross-talk with the growth hormone auxin (5, 6). Ethylene-associated changes in plant architecture frequently function as adaptations to the environment or as part of survival. For instance, seedlings germinating underground form a shorter and thicker stem and a hook-like structure, assisting the seedling to emerge without damaging the shoot meristem, a process regulated by ethylene (7, 8).

Hormones control organ growth by regulating specific growth processes (cell division, expansion, or differentiation) in distinct tissues (9). Cell type-specific interference with hormone signaling has been successfully applied to map the cell types that are important for positive control of growth in *Arabidopsis* roots and shoots. The site of action of different hormones can mainly be accounted for by single cell types: the endodermis for gibberellins (GAs) (10, 11), the epidermis for auxins (12) and brassinosteroids (BRs) (13, 14), and cortical cells for abscisic acid (15). However, the tissues where the major elongation inhibitory hormone ethylene is perceived and generates a response remain still elusive. Previously, Swarup et al. (16) used cell type-specific expression of the auxin influx carrier AUXIN1 (AUX1) and a mutant form of the AUXIN/INDOLE-3-ACETIC ACID17 (AUX/IAA17) repressor protein, *axr3-1*, to determine in which tissues ethylene mediated its effects on auxins to control cell growth. The current model of ethylene action on root growth proposes that ethylene stimulates auxin biosynthesis in the root tip and that effects of ethylene require auxin transport in the lateral root cap (LRC) and epidermis by AUX1 and PIN-FORMED 2 (PIN2) (16, 17). The present work aimed to identify the cell types in which ethylene needs to be perceived to exert its growth-inhibitory function.

The transcription factors ETHYLENE INSENSITIVE 3 (EIN3) and ETHYLENE INSENSITIVE LIKE 1 (EIL1) are key ethylene signaling components (18, 19) controlling the expression of ethylene response genes. Both members of the ethylene signaling cascade, EIN2 and EIN3, interact with EIN2 NUCLEAR ASSOCIATED PROTEIN 1 (ENAP1), which controls histone acetylation and has been linked to an EIN2-dependent enhancement of ethylene-inducible gene expression (20). EIN3 and EIL1 are degraded in a 26S proteasome pathway mediated by ubiquitin E3 ligases containing the EIN3 BINDING F-BOX proteins EBF1 and EBF2 (21–23). Recently, it was proven that the EIN2 C-terminal end participates in modulating the degree of translation of the two F-box proteins by targeting their mRNA to cytoplasmic processing bodies (24, 25). In this regard, the targeted EBF1/EBF2 expression presents an effective approach to establish cell type-specific insensitivity to ethylene, thereby revealing the necessity of the ethylene signal in a given cell type to steer elongation growth.

Significance

Ethylene is a gaseous hormone that controls plant life throughout development. Being a simple hydrophobic molecule, it can freely enter cells; therefore, the cell type specificity of its action is challenging. By means of tissue-specific expression of two negative regulators of the signaling cascade, we selectively disrupted the ethylene signal in different cell types without affecting its biosynthesis. We demonstrate that ethylene restricts plant growth by dampening the effect of auxins in the outermost cell layer. We further show that this epidermis-specific signaling has an impact on the growth of neighboring cells, suggesting that the master controller of cell expansion resides in the epidermis, where it senses the environment and, subsequently drives growth, of the inner tissues.

Author contributions: I.I.V., T.P., P.G., F.V., and D.V.D.S. designed research; I.I.V., E.Q., T.P., Y.D., and F.V. performed research; I.I.V., E.Q., T.P., Y.D., P.G., F.V., and D.V.D.S. analyzed data; I.I.V. and D.V.D.S. wrote the paper; and D.V.D.S. conceived and coordinated the project.

The authors declare no conflict of interest.

This article is a PNAS Direct Submission.

[1]Present address: Institute of Plant Physiology and Genetics, Laboratory Regulation of Gene Expression, Bulgarian Academy of Sciences, Sofia 1113, Bulgaria.

[2]Present address: Center for Genomics and Systems Biology, New York University Abu Dhabi, Abu Dhabi, United Arab Emirates.

[3]Present address: State Key Laboratory for Conservation and Utilization of Bio-Resources in Yunnan, Yunnan Agricultural University, Kunming 650201, China.

[4]To whom correspondence should be addressed. Email: dominique.vanderstraeten@ugent.be.

This article contains supporting information online at www.pnas.org/lookup/suppl/doi:10.1073/pnas.1717649115/-/DCSupplemental.

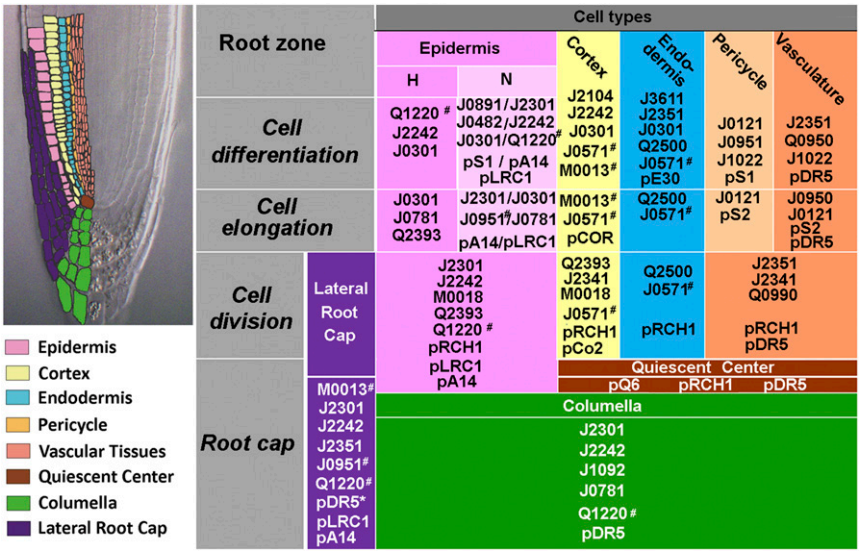

Fig. 1. Overview of the cell type-specific promoters used to drive the expression of EBF1/EBF2 F-box proteins in the different root cell types. The legend with color-coded root cell types is prepared according to Barrada et al. (26). The asterisk indicates that the promoter is ethylene-inducible in the particular cell type. Promoters marked with # were also used by Swarup et al. (16). H, trichoblasts; N, atrichoblasts.

Results

We used a number of cell type-specific promoters (26) (listed in Fig. 1) coupled to EBF1 and EBF2 as effectors. The choice of EBF effectors was carefully considered. Given the feedback control mechanisms operating in the ethylene pathway, leading to hormone overproduction when ethylene signaling is shut down (5, 27), dominant negative interference with the ethylene response should occur without affecting its biosynthesis, thus avoiding non–cell-autonomous effects in adjacent cell types. Overexpression of EBF1 or EBF2 results in an ethylene-insensitive root phenotype (Fig. 2*A*) and suppresses expression of the ethylene reporter *pEBS::GUS* (Fig. 2*B*). However, in contrast to the strong increase in ethylene production observed in the ethylene-insensitive mutant *ein2-1*, also seen for the ethylene-insensitive receptor mutant *etr1-1* (5), EBF1/2 overexpressing lines do not emit excessive ethylene (Fig. 2*C*). Hence, EBFs are suitable targets for ethylene signal interference. We implemented their cell type-specific expression to selectively block ethylene signaling through EIN3 degradation in specific cell types.

Targeted Expression of EBF1/2 Reveals That Ethylene Controls both Root and Shoot Elongation via the Epidermis. Transactivation using GAL4-GFP enhancer trap lines driving the expression of an effector construct in particular cell types under the control of the yeast upstream activator sequence (UAS) has been successfully applied for dominant interference with hormonal responses (10, 12). We used the Gal4:VP16/UAS transactivation system (28) to perform a broad screen to identify driver lines (in C24 background) capable of inducing ethylene insensitivity when activating the *UAS::EBF1* construct (crossing and direct transformation data, including root lengths of the different lines, are shown in *SI Appendix*, Fig. S1 *A* and *B* and Tables S1 and S2, respectively). Among 24 driver lines with distinct expression patterns, only those expressing EBF1 in the LRC and epidermis (J2301, J0951, and Q1220; *SI Appendix*, Fig. S1) had a longer root phenotype than the controls on media supplemented with the ethylene precursor 1-aminocyclopropane-1-carboxylic acid (ACC). These results indicate cell type-specific alteration of ethylene-sensitive root growth. Due to the generally low expression levels of the promoters, or possible participation of other root cell types, none of the driver-effector combinations conferred complete ethylene insensitivity (*SI Appendix*, Fig. S1). Furthermore, disruption of ethylene signaling in the root maturation zone alone did not confer ethylene insensitivity (J0301 and J0482; *SI Appendix*, Fig. S1*A* and J0121, Q0950, and J2104; *SI Appendix*, Fig. S1*B*). Most of the GAL4 driver lines used for our initial screen targeted the expression of EBFs in a combination of root cell types.

For more restrictive targeting of the EBFs, we employed cell type-specific root promoters selected according to their GFP

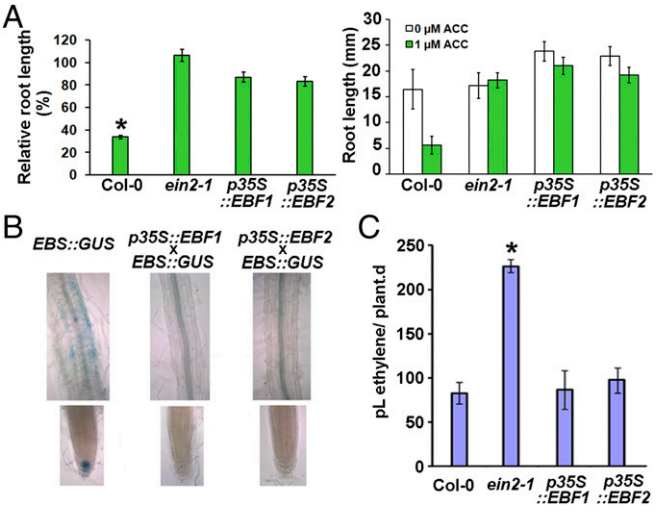

Fig. 2. EBF1/2 overexpression affects the ethylene signaling pathway without interfering with ethylene biosynthesis. (*A*) Roots of 6-d-old seedlings exhibit strong resistance to ACC treatment when EBF1/2 is overexpressed. Error bars indicate SD ($n = 20$, results are from one representative experiment). Absolute root length (*Right*) (millimeters; results obtained from a single experiment) is shown next to the relative values (*Left*). *$P \leq 0.05$ (Welch's *t* test) vs. control plants from the same genotype grown on media without ACC. (*B*) Bright-field micrographs of GUS-stained wild-type and F1 *p35S::EBF1/2* seedlings carrying the *pEBS::GUS* reporter gene, grown for 6 d on 1/2 MS medium in the presence of 1 µM ACC. (Magnification: 20×.) (*C*) Ethylene production by Col-0, *ein2-1*, and *p35S::EBF1/2* (expressed as picoliters of ethylene produced by a single individual over a period of 24 h). Error bars indicate SD ($n \geq 3$, each independent sample contained 100 seeds grown in a sealed cuvette). *$P < 0.05$ vs. control (Col-0), assessed by Welch's *t* test.

reporter expression patterns (Fig. 3*A*), fused with EBF1 and/or EBF2 coding sequences, and transformed into Col-0 wild-type background. Transgenic plants (lists of the evaluated lines are provided in *SI Appendix*, Tables S3 and S4) were scored for ethylene insensitivity of the primary root on medium containing 1 μM ACC (Fig. 3*B* and *SI Appendix*, Fig. S1*C*; absolute root lengths are shown in *SI Appendix*, Fig. S2*A*). Transformation with *pA14::EBF1* (*SI Appendix*, Fig. S1*C*) resulted in modest ethylene insensitivity (relative root length reaching 50% on ACC-containing medium compared with control), while *pA14::EBF2* lines (Fig. 3*B*) had a stronger ethylene-insensitive phenotype, with relative root elongation reaching 70% of the length of the untreated control. In contrast, constructs driving EBF expression in the stele (*pS2::EBF1/EBF2*), quiescent center (QC) (*pQ6::EBF1*), and columella (*pDR5::EBF2*) did not confer root ethylene insensitivity (Fig. 3*B* and *SI Appendix*, Fig. S1*C*). Similarly, lines in which ethylene signaling was reduced in the epidermis and pericycle in the late elongation zone (EZ; *pS1::EBF1/EBF2*) or in the endodermis of the differentiation zone (DZ; *pE30::EBF1/EBF2*) (Fig. 3*A*) also did not confer ethylene insensitivity (Fig. 3*B* and *SI Appendix*, Fig. S1*C*). Root ethylene insensitivity of the transgenic lines was further validated by treatment with ethylene gas (*SI Appendix*, Fig. S3*A*). Taken together with the observations using the GAL4-UAS system, where driver lines expressing EBF1 only in the differentiation zone failed to exhibit a phenotype, we conclude that EBF expression in the root differentiation zone is not sufficient to interfere with the ethylene-regulated root elongation. To verify the functionality of these constructs, we developed a *pEIN3::gEIN3-3xGFP* (*ein3-1*) reporter line (*SI Appendix*, Fig. S4). Homozygous transgenic lines expressing EBFs in a cell type-specific manner were crossed with the reporter. Characterization of the GFP expression pattern in F1 plants allowed monitoring the changes in EIN3 abundance triggered by targeted expression of the EIN3 F-box proteins (Fig. 3*C*). F1 plants exhibited loss of the GFP signal in the tissues where the ethylene signal was suppressed by cell type-specific expression of EBFs (Fig. 3*C* and *SI Appendix*, Fig. S4). The crosses between the reporter and transgenic lines with targeted F-box protein expression in the LRC and epidermis of cell division and elongation zone (CDZ and EZ, respectively)

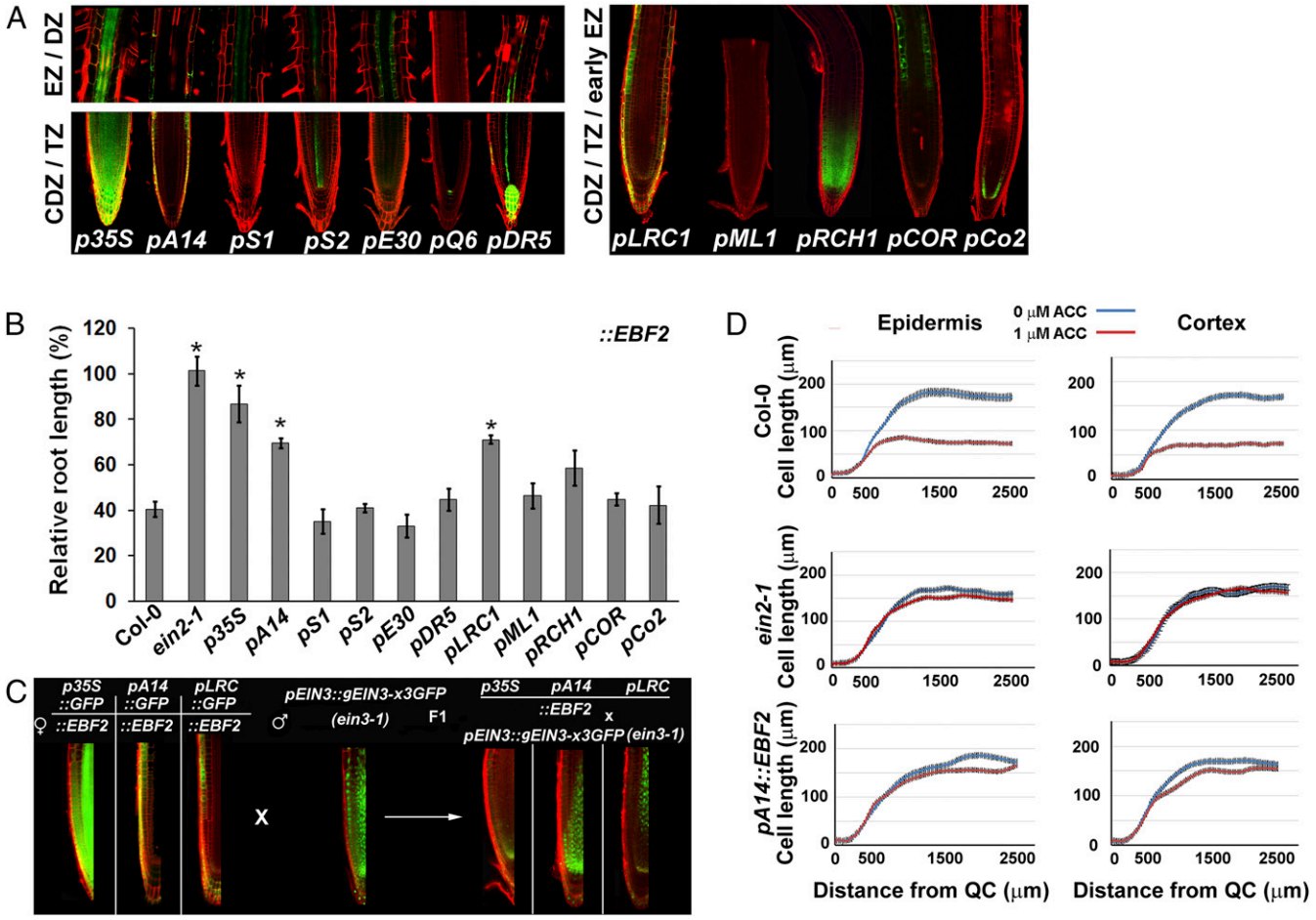

Fig. 3. Targeted cell type-specific expression of EIN3-binding F-box protein EBF2 reveals that ethylene signaling in the LRC and epidermis controls root elongation. (*A*) Confocal images of *promoter::GFP* reporter lines grown in the presence of 1 μM ACC, visualizing the expression pattern of the selected root cell type-specific promoters fused to EIN3-binding F-box proteins in different root zones: cell division zone (CDZ), transition zone (TZ), elongation zone (EZ), and differentiation zone (DZ). (Magnification: 20×.) (*B*) Relative root length of different lines on 1/2 MS medium containing 1 μM ACC compared with medium without ACC. Error bars indicate SD ($n = 3$ datasets). *$P \leq 0.05$ (Welch's t test with Holm–Bonferroni sequential correction) reflects the significant differences in relative growth on ACC. (*C*) F1 crosses of the transgenic plants carrying constructs with cell type-specific expression of the F-box protein with the reporter *pEIN3::gEIN3-3xGFP* (*ein3-1*) confirmed the functionality of the constructs. The specific promoter-driven EBF lines used as mother plants did not contain a GFP reporter; the images of *promoter::GFP* depicted here are as in *A* and only visualize the expression pattern. Zoomed-in sectors of confocal images are shown. (Magnification: 20×.) (*D*) Inhibition of root cell elongation by ACC is relieved when the ethylene signal is blocked in the LRC and epidermis. Profiles of root epidermal and cortical cell expansion in wild type (Col-0), *ein2-1* ethylene-insensitive mutant, and a transgenic line with epidermis- and LRC-targeted EBF2 expression (*pA14::EBF2*).

(*pA14::EBF2* and *pLRC1::EBF2*) exhibited reduced fluorescent EIN3-GFP signal, confirming the presence of functional EBF2 therein (Fig. 3*C*). Ethylene signaling in the root CDZ and EZ was further assessed by promoters active in various cell types: *pCo2* (cortex initials), *pCOR* (cortex promoter, active only in the EZ), *pRCH1* (covering all cell types of the root apical meristem, but weakly expressed in the LRC), and *pLRC1* (active in the LRC and epidermis) (Fig. 3*A*). The strong shoot but weak root epidermal promoter *pML1* (Fig. 3*A* and *SI Appendix*, Fig. S5) was tested in parallel. Transgenic plants carrying *pLRC1::EBF2* (LRC and epidermis) exhibited strong ethylene insensitivity in our ACC root inhibition bioassay, comparable to the *pA14::EBF2* line (Fig. 3*B*). The root apical meristem (RAM) promoter *pRCH1*, with low expression in the LRC, conferred partial ethylene insensitivity, although significantly weaker than that observed in the "LRC + epidermis" constructs *pA14::EBF2* and *pLRC1::EBF2* (Fig. 3*B*). To assess whether the effect of LRC/epidermis-specific expression of EBF2 in the root is also reflected at the cellular level, we measured root epidermal and cortical cell lengths of wild-type and *pA14::EBF2* plants in the absence and presence of ACC, with *ein2-1* as a control. Col-0 revealed that the growth inhibition caused by 1 μM ACC correlated with ∼60% reduction in mature cell length (Fig. 3*D*). In contrast, the ethylene signaling mutant *ein2-1* did not show reduced cell elongation of mature cells when grown on ACC-supplemented media (Fig. 3*D*). The transgenic plants (*pA14::EBF2*) in which the ethylene signal was blocked in the LRC and epidermis also failed to exhibit a reduction in mature cell length upon ACC treatment (relative cell length reaching 93%), supporting the primary significance of these cell types for the ethylene-driven inhibition of root elongation, while also reflecting the effect of epidermal expression on the adjacent cell layer.

Given that epidermal ethylene signaling is of major significance in the root, we subsequently checked whether this tissue also controls ethylene-regulated shoot growth. The importance of the epidermis for regulation of leaf growth has been described for BRs (13). Shoot growth of *pML1::EBF2*, *pA14::EBF2*, and *pLRC1::EBF2* transgenic lines was assessed in the presence of increasing concentrations of ACC (*SI Appendix*, Fig. S2*B*), and the results were validated by treatment with ethylene gas (*SI Appendix*, Fig. S3*B*). Engineering an ethylene signaling deficiency in the leaf epidermis rendered seedlings insensitive toward ACC treatment in a dose-dependent manner (*SI Appendix*, Fig. S2*B*). Even at a saturating concentration (50 μM ACC), lines with disrupted responses in the leaf epidermis (*pML1::EBF2* and *pLRC1::EBF2*) remained partially ethylene-insensitive, able to grow relatively large rosettes compared with the wild type (Fig. 4*A*). In contrast, the *pA14::EBF2* line, which exhibited limited expression of the transgene in the shoot epidermis, did not confer ethylene-insensitive leaf growth (Fig. 4*A*). Similar results were obtained when these lines were treated with ethylene gas (*SI Appendix*, Fig. S3*B*). Differential interference contrast (DIC) microscopy of cleared leaves revealed that the growth differences at the level of rosettes were also reflected at the level of leaf epidermal cell expansion (Fig. 4*B*). The pavement cells of the transgenic lines with reduced ethylene signaling in the epidermis showed strong ACC insensitivity, while *pA14::EBF2* exhibited weaker, although still significant, insensitivity (Fig. 4*B*).

Reduced Ethylene Signal in the Epidermis Functionally Complements the *ctr1-1* Mutation. CONSTITUTIVE TRIPLE RESPONSE1 (*ctr1*) loss-of-function mutation results in plants with a dwarfed rosette, very short roots, and excessive formation of ectopic root hairs even in the absence of ACC or ethylene. Transformation of *ctr1-1* with the *pLRC1::EBF2* construct, which triggers F-box protein expression in both the shoot and root epidermis, rescued the mutant phenotype (Fig. 4*C*). Partial complementation of *ctr1-1* was obtained by *pA14::EBF2* in roots but not in shoots,

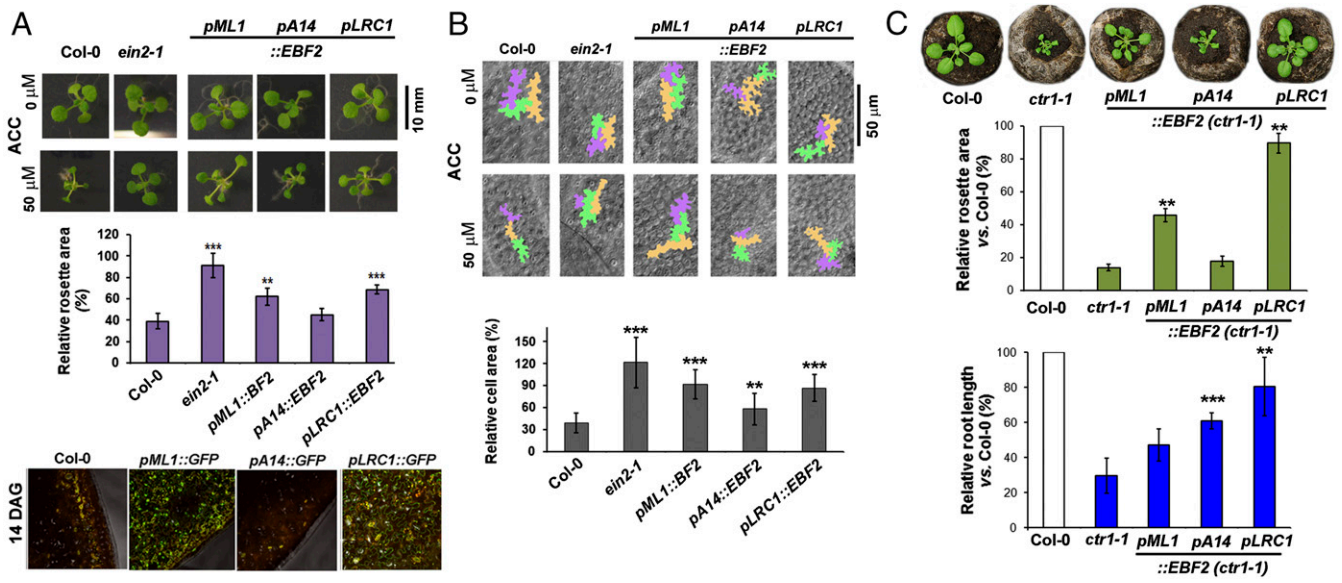

Fig. 4. Epidermis-specific suppression of the ethylene signal positively influences cell expansion in leaves and complements *ctr1-1*. (*A*) Light-grown 14-d-old seedlings with compromised ethylene signaling in leaf epidermis (*pML1::EBF2* and *pLRC1::EBF2*) are insensitive to ACC. Error bars represent SD ($n = 3$ datasets). $^{**}P \leq 0.01$; $^{***}P \leq 0.001$ (Welch's *t* test with Holm–Bonferroni sequential correction). Confocal images of the first true rosette leaves of *pML1::GFP*, *pA14::GFP*, and *pLRC1::GFP* at 14 DAG (days after germination). A wild-type Col-0 shoot was used as a control for autofluorescence correction. (Magnification: 20×.) (*B*) Leaf pavement cell area of ethylene-insensitive lines shows reduced response to treatment with 50 μM ACC. DIC microscopic observations are made on cleared first true leaves at 21 DAG. Three neighboring cells are artificially colored to visualize the differences between the controls and the treated samples. Error bars indicate SD ($n \geq 20$). $^{**}P \leq 0.01$; $^{***}P \leq 0.001$ (Welch's *t* test with Holm-Bonferroni sequential correction). (*C*) Root elongation assay, phenotype, and rosette area of *ctr1-1* transgenic lines carrying *pLRC1::EBF2* (strong root and shoot epidermal promoter), *pML1::EBF2* (weak root and strong shoot epidermal promoter), or *pA14::EBF2* (strong root and weak shoot epidermal promoter) constructs. Error bars indicate SD ($n = 3$ datasets). Statistically significant difference with *ctr1-1*: $^{*}P \leq 0.05$; $^{***}P < 0.001$ (Welch's *t* test with Holm–Bonferroni sequential correction).

consistent with its weak expression in the aerial plant parts, and by *pML1::EBF2*, which is a strong shoot epidermal promoter (Fig. 4*A* and *SI Appendix*, Fig. S5). Genotyping confirmed the mutant background of the transgenic plants with a rescued phenotype (*SI Appendix*, Fig. S6).

The Inhibition of Plant Growth by Ethylene Is Achieved by Control of Local Auxin Biosynthesis and Transport in the Epidermis. The well-established stimulatory effect of ethylene on auxin biosynthesis and distribution (16, 17, 29) implies that any disturbance of ethylene signaling could affect auxin homeostasis. Part of the strict maintenance of endogenous auxin levels relies on the regulation of expression of indole-3-acetic acid (IAA) biosynthetic genes through a negative feedback mechanism (30). It has been previously reported that ethylene controls auxin biosynthesis by inducing the genes encoding the two subunits of anthranilate synthase, the rate-limiting step in accumulation of tryptophan, a major precursor of IAA (29–31). Likewise, the gene encoding TRYPTOPHAN AMINOTRANSFERASE1 (TAA1), an essential component of the indole-3-pyruvic acid (IPA) branch of the auxin biosynthetic pathway, is under ethylene control (32). Moreover, a recent study proposed involvement of ethylene in the TAA1-regulated local auxin response in the transition zone (TZ) (33). We used the *pTAA1::GFP-TAA1* reporter (32) to visualize the effect of cell type-specific interference with ethylene signaling on local auxin biosynthesis. The experiments were performed with the strong epidermal root promoters *pLRC1* and *pA14*, which were capable of complementing the *ctr1-1* mutation when fused to EBF2. Treatment with the IAA biosynthetic inhibitor kynurenine (Kyn), which competitively inhibits TAA1/TRYPTOPHAN AMINOTRANSFERASE RELATED PROTEIN (TAR) function (31), in combination with ACC, shows

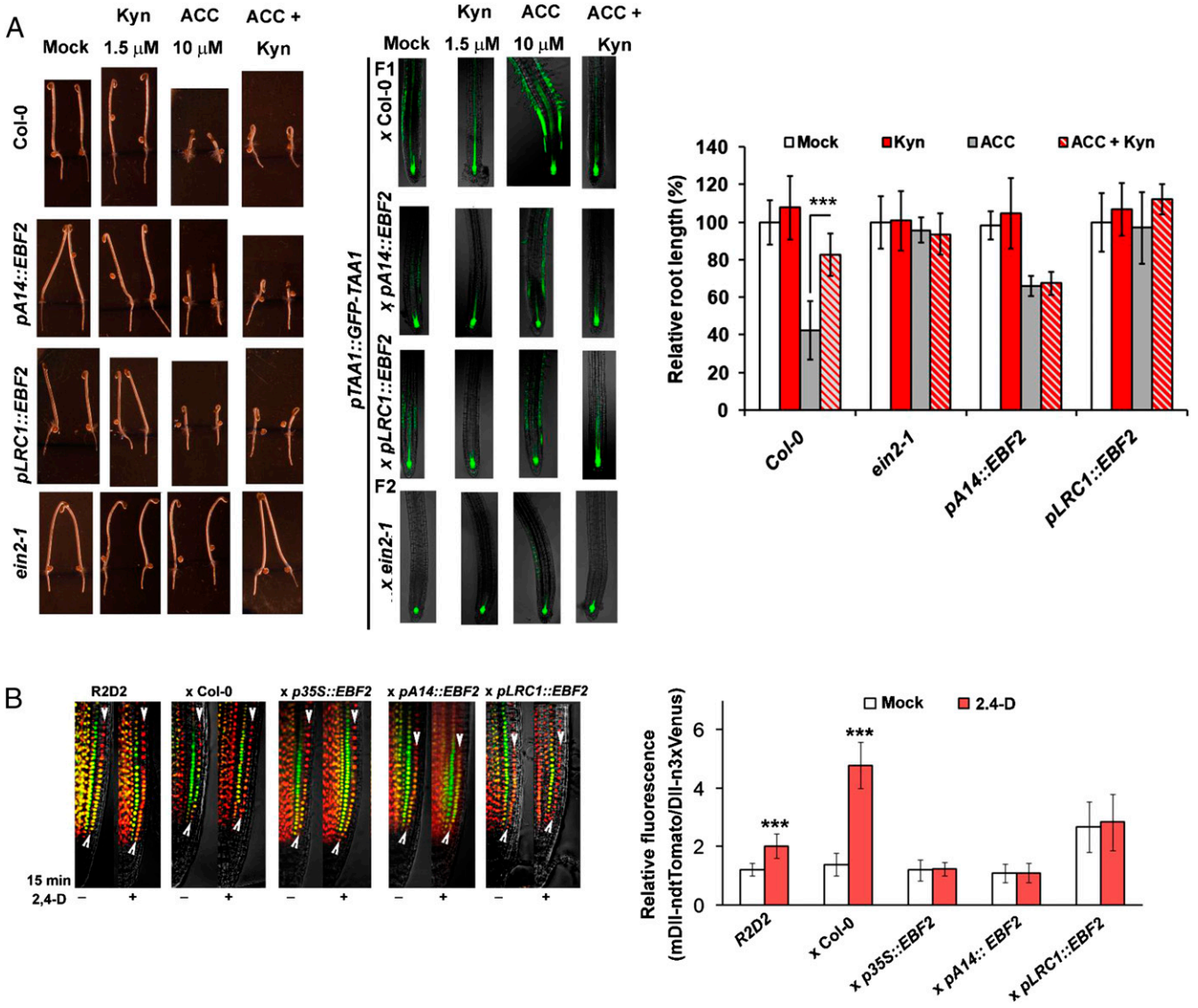

Fig. 5. Reduced ethylene signal in the LRC and epidermis affects auxin biosynthesis and responsiveness in the root tip. (*A*) Reduction of root growth by ACC in dark-grown seedlings is abolished by application of the auxin biosynthetic inhibitor L-Kyn (Kyn). Statistically significant differences between ACC and ACC + Kyn-treated individuals: ***$P \leq 0.001$ (Welch's *t* test). Error bars represent SD ($n \geq 20$). Crosses between the translational fusion reporter line *pTAA1::GFP-TAA1* and the ethylene-insensitive transgenic lines *pA14::EBF2* and *pLRC1::EBF2* reveal that EBF2 cell type-specific expression in the epidermis and LRC impairs ethylene responsiveness of TAA1 expression therein. (Magnification: 20×.) (*B*) Cells with reduced ethylene signaling have altered responsiveness to 50 nM 2,4-D short-term treatment. Error bars represent SD ($n \geq 20$). Statistically different results are shown: ***$P \leq 0.001$ (Welch's *t* test). White arrowheads on the representative confocal images mark the epidermal cell files where the measurements are taken. (Magnification: 40×.)

that an increased level of auxin in the epidermis is linked to reduced root elongation in response to ACC (Fig. 5*A*, compare *pTAA1::GFP-TAA1* pattern and relative root growth values). The root response of the ethylene-insensitive mutant *ein2-1*, *pA14::EBF2*, and *pLRC1::EBF2* lines toward both ACC and Kyn treatments was similar, which suggests impaired regulation of local auxin biosynthesis in these plants (Fig. 5*A*). The crosses of the reporter *pTAA1::GFP-TAA1* (32) with *pA14::EBF2*, *pLRC1::EBF2*, and *ein2-1* led to a strong suppression of the epidermal signal upon treatment with ACC, compared with the wild type (Fig. 5*A*).

Next, we evaluated the responsiveness of the EBF2-targeted cells to auxins by crossing the transgenic lines with the auxin sensor R2D2 (34) and monitoring the effect of short-term treatment with 2,4-D on F1 crosses (Fig. 5*B*). A diminishing green fluorescent signal in R2D2 reflects higher auxin levels, as the conserved domain II (DII) marker (*RPS5A*-driven DII fused to n3×Venus) is rapidly degraded in response to auxin, while *RPS5A*-driven mutated DII fused to ntdTomato, allows ratiometric quantification of the changes in fluorescence. The synthetic auxin 2,4-D is actively imported in cells but is not exported by efflux transporters. Upon treatment, intracellular accumulation of 2,4-D was manifested by a considerable decrease of the green fluorescent signal of the R2D2 reporter. In contrast, epidermal cells in the crosses with *pA14::EBF2* and *pLRC1::EBF2* remained unresponsive to 2,4-D treatment, suggesting impaired response of Aux/IAA proteins due to the reduced ethylene signaling (Fig. 5*B*). Similarly, the ethylene-insensitive lines showed a reduced response toward exogenous auxin compared with the wild type when grown for 6 d on media supplemented with 100 nM IAA (*SI Appendix*, Fig. S7).

Auxins often act in sites remote from their place of synthesis; therefore, their activity also depends on the distribution via nonpolar (phloem) and polar (intercellular) transport (35). Mutation of the auxin influx carrier AUX1 confers insensitivity toward both auxins and ethylene (36). Previous studies have reported that ethylene up-regulates AUX1 (17, 37); hence, blocked ethylene signaling in the cells where AUX1 operates will interfere with the polar auxin transport. Interestingly, in roots, *AUX1* has an expression pattern similar to *pA14* and *pLRC1* promoters [i.e., in the LRC and epidermal atrichoblasts, as visualized by the reporter line *pAUX1::AUX1-YFP* (*aux1-22*)] (38, 39) (Fig. 6*A*). To test the relationship between the cell type-specific ethylene signaling and auxin transport, we crossed the ethylene-insensitive transgenic lines *pA14::EBF2* and *pLRC1::EBF2* with the strong recessive mutant *aux1-22* (38) and evaluated the ethylene sensitivity of the F2 individuals with *aux1* phenotype (Fig. 6*A*), easily distinguishable by their agravitropic roots (*SI Appendix*, Fig. S8). As the *aux1* mutation did not have an additive effect on the root elongation of the lines with ethylene insensitivity, AUX1 and ethylene are likely acting in one and the same regulatory pathway in the outermost layers. This was further confirmed in the F1 crosses of the ethylene-insensitive lines with the reporter *pAUX1::AUX1-YFP* (*aux1-22*). Whereas in the cross with wild type, AUX1 levels were increased in the presence of ACC, this was not the case in *pA14::EBF2* and *pLRC1::EBF2* background, suggesting that disturbance of the ethylene signal prevents the induction of the auxin importer (Fig. 6*A*). In addition, these plants demonstrated obstructed auxin efflux since crosses with *pPIN2::PIN2-GFP* (*pin2*) reporter (40) showed that *pPIN2* activation was reduced upon ACC treatment (Fig. 6*B*).

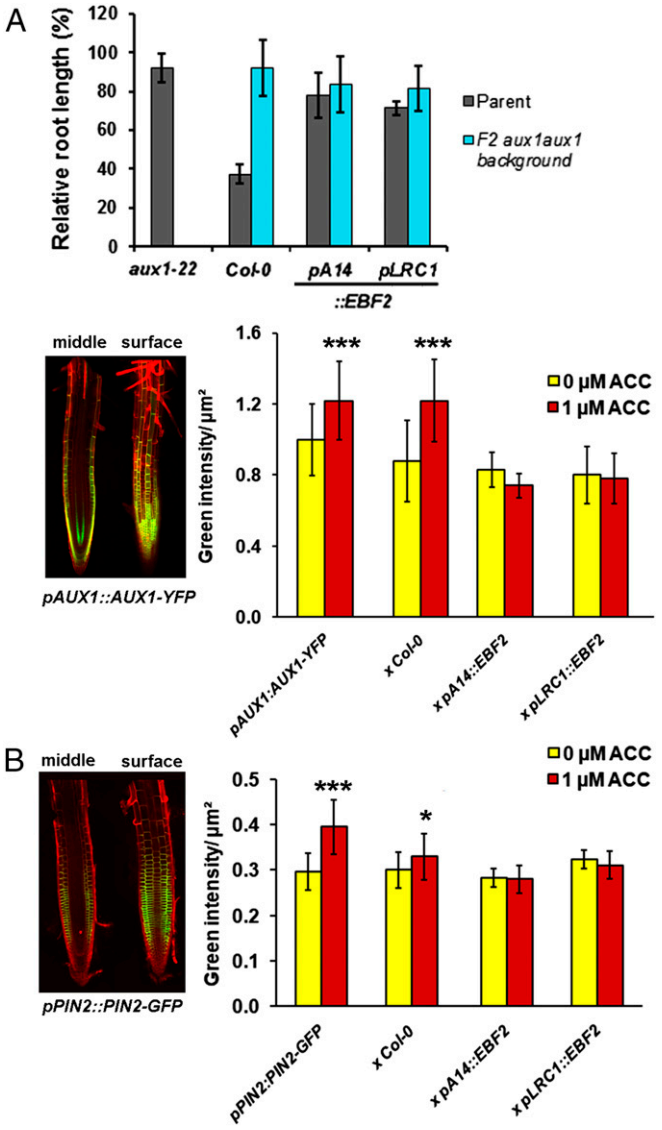

Fig. 6. Reduced ethylene signal in the LRC and epidermis affects auxin transport in the root tip. (*A*) Attenuation of ethylene signals in the LRC and epidermis abolishes the positive effect of ethylene on basipetal auxin transport. The reduced root elongation by ACC is at least partially dependent on functional AUX1 as evident from the F2 crosses between the recessive *aux1-22* null mutant and the transgenic lines with LRC + epidermis-specific EBF2 expression (*pLRC1::EBF2* and *pA14::EBF2*). Relative root lengths of F2 with *aux1* background grown for 6 DAG in the presence of 1 μM ACC is shown. Error bars represent SD ($n \geq 4$ datasets from independent crosses). Relative green intensity in the LRC of F1 crosses between the auxin transport reporter *pAUX1::AUX1-YFP* (confocal image at 20× magnification) and the wild type (Col-0) or transgenic line confirms that the ethylene-insensitive line has altered auxin import. (*B*) PIN2 is expressed in the cortex and epidermis of the root cell division zone and EZ, as it is visualized in the confocal image (20× magnification) of the reporter line *pPIN2::PIN2-GFP* (*pin2*). Relative green intensity at the middle optical section in roots of 1 μM ACC-treated seedlings vs. untreated control was measured in F1 crosses. Error bars are SD ($n \geq 10$). Statistical significance between the control and the ACC-treated plants: $^{*}P \leq 0.05$; $^{***}P \leq 0.001$ (Welch's *t* test).

Discussion

The outermost cell layer of plant organs is in constant contact with the surrounding environment, thus being the first cell layer to encounter the effects of external cues, such as nutrient availability, humidity, and light. At the root level, the root cap also acts as a sensor to perceive these signals and transmit the information to the root TZ, which subsequently triggers responses in the EZ (41, 42). The root TZ has been proposed to function as a control center for cell growth and cell fate switches (43, 44). Hence, although the in silico characterization of expression profiles reflects a fairly uniform expression of ethylene receptors and signaling genes throughout all root tissues (45), the leading role of the epidermis in

stress signal perception and transmission to the inner cell layers is a logical consequence.

Growth inhibition by ethylene occurs through complex cross-talk with other phytohormones, among which auxin has been considered as a primary partner. Despite the fact that a clear requirement for auxins in the tissues of the EZ was demonstrated (16), the exact mechanism of the cross-talk with ethylene in controlling cell expansion remained vague. It has been proposed that through auxin modulation, ethylene is capable of specifically inhibiting growth of expanding cells (16, 46) or reducing cell proliferation (47). In *Brachypodium*, ethylene was suggested to confer suboptimal auxin levels for root cell elongation by inhibiting the rate-limiting step of auxin biosynthesis in the IPA pathway (48), one of the major pathways leading to accumulation of IAA in plants, involving TAA1 action (49, 50). In *Arabidopsis*, root growth inhibition caused by Al toxicity was linked to TAA1-regulated auxin biosynthesis in the TZ and found to be dependent on ethylene (33).

As demonstrated by Swarup et al. (16), ethylene-regulated root growth is dependent on transport of auxin from the root apex via the LRC to expanding epidermal cells. Here, we show that the ethylene signal perceived in the LRC and epidermis influences root growth by affecting local auxin biosynthesis through the TAA1 pathway in elongating epidermal cells, along with fine-tuning basipetal AUX1-dependent transport of auxin in the LRC and epidermis, confirming the critical role of these tissues for the effects of ethylene. Stepanova et al. (29) observed that the roots of several auxin mutants (*wei2*, *aux1*, *eir1/pin2*, *axr1*, and *tir1*) show significant ACC insensitivity, while ethylene mutants (*ein2*, *ein3*, and *eil1*) are sensitive toward exogenous auxin. Together with their mutual transcriptional regulation of biosynthesis genes [reviewed by Vandenbussche et al. (5)], this strongly suggests the existence of a reciprocal regulatory loop, with several levels of interaction.

According to the proposed model (Fig. 7), ethylene signals in the root epidermis relieve the suppression exerted by CTR1 on the downstream ethylene signaling component EIN2, which itself translationally controls EBF1/2 to degrade EIN3 and EIL1 transcription factors (24, 25). AUX1 and PIN2, as well as TAA1, which is involved in local auxin biosynthesis, are operating in the root epidermis and are targets for positive regulation by EIN3/EIL1 (20). The resulting altered auxin balance in root TZ cells prevents their elongation, which is reflected in the overall root growth. Our findings also support a positive interference of ethylene signaling on AUX/IAA repressors (Figs. 5*B* and 7). It should be noted that the regulation of expression of *AUX1* and *PIN2* by ethylene, also observed by Růzicka et al. (17), is relatively weak, and therefore unlikely to play a substantial role in regulating auxin transport, which could be controlled by ethylene at the posttranslational level.

The multilevel regulatory role of ethylene on auxin homeostasis suggests that it has a leading function in the hormonal network that dampens root elongation growth. The recent work of Barbez et al. (51) suggests a model in which auxin plays a concentration-dependent role in apoplastic pH homeostasis during root growth. This is consistent with previous literature (52–56) reporting that low auxin concentrations stimulate and high auxin concentrations inhibit root growth, corresponding to apoplastic acidification and alkalization, respectively. Interestingly, it was also shown that fast cell elongation is inhibited within minutes by the ethylene precursor ACC, concomitant with apoplastic alkalinization in the affected root zone (57). Staal et al. (57) demonstrated that in *Arabidopsis* roots, the surface pH drops substantially from the meristem/TZ boundary toward the EZ. In accordance with this, treatment of maize roots with auxin, combined with exposure to ethylene inhibitors, strongly promoted growth, preceded by enhanced acidification (58). Hence, based on previous evidence (16, 17, 51, 57) and this work, we propose an integrative model in which ethylene, perceived in the epidermis of the TZ, coregulates the apoplastic pH through its control over the cellular auxin level, restricting elongation growth (Fig. 7).

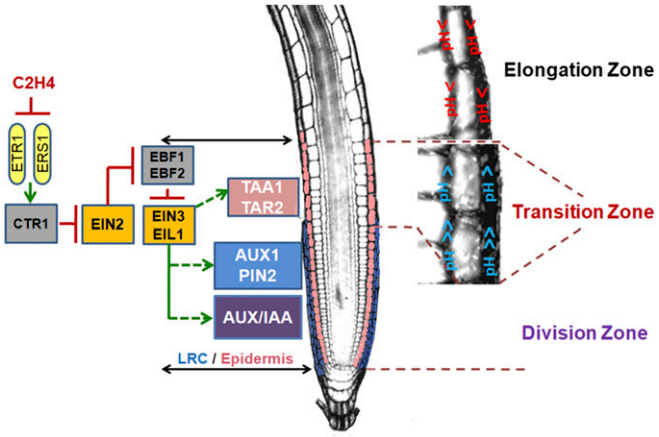

Fig. 7. Integrative model of ethylene feedback on auxin homeostasis in the root tip. Ethylene perceived in the LRC and epidermis of the cell division zone regulates root growth by positive control on auxin transport and local auxin biosynthesis in the TZ. Ethylene signals perceived in the root tip relieve the suppression of CTR1 on EIN2 and EIN3/EIL1. AUX, PIN2, AUX/IAA, and TAA1 in the LRC and epidermis are indirect targets for positive regulation by EIN3/EIL1. Surface pH drops from the meristem/TZ boundary toward the zone of fast elongation (57). Low auxin concentrations stimulate and high auxin concentrations inhibit root growth, corresponding to apoplastic acidification and transient alkalinization, respectively (51), while ethylene causes growth inhibition concomitant with apoplastic alkalinization (57). Hence, through its control over auxin levels, ethylene restricts elongation growth. The symbols > and < indicate relatively higher and lower pH values compared with the adjacent zones. The model is based on findings reported elsewhere (16, 17, 51–57) and in this work.

The current study confirms that ethylene induces auxin transport from the root apex via the LRC and epidermis (16, 17, 37). Moreover, our results substantiate the cell type specificity of hormonal control of root growth by demonstrating that auxin levels in the epidermis are controlled by ethylene signaling therein, with the TZ acting as a determinant output site for the cross-talk between the two hormones. Furthermore, Swarup et al. (16) suggested that the ethylene effects through auxin above the lateral root cap in the EZ require multiple cell types to observe a maximal effect on growth. This conclusion was based on targeted expression of a dominant negative form of the auxin signaling repressor AXR3/IAA17, *axr3-1*, using a transactivation approach. Strong resistance was found when *axr3-1* was expressed in all EZ tissues [using the J0631 driver line (28)], while only weak resistance was conferred when targeted to the epidermis. A major difference between these earlier findings and the present study is that the current work directly maps the site of ethylene action by using an effector within the signaling pathway itself, while the approach of Swarup et al. (16) involves a factor in auxin signaling. Ethylene particularly acts on the steps before auxin signaling occurs (namely, the biosynthesis and redistribution of auxin). In conclusion, the results of Swarup et al. (16) may rather indicate an indirect effect on ethylene action, for instance, related to lateral auxin redistribution from the epidermis within the cortex and inner tissues, that is driven, among other factors, by auxin itself (29).

Furthermore, our results also provide evidence that the epidermis is of primary importance in the control of cell expansion in shoots. This is supported by the fact that suppression of ethylene signaling in expanding epidermal cells complemented the *ctr1-1* mutation and rescued not only its root but also its shoot phenotype. This cell type-specific inhibitory role of ethylene is, to

our current knowledge, unique. It reveals ethylene as a central negative regulator of the feedback loop that drives elongation by imposing a brake on auxin action in the epidermis.

Importantly, epidermis-specific control by ethylene clearly has an impact on the cortical cell layer, coordinating its growth together with the outer layer (Fig. 3*D*). Hence, we provide experimental evidence of the model, predicting that the master controller of root expansion resides in the epidermis (59), where it senses the environment both in the rhizosphere and the phyllosphere, and subsequently drives growth of the inner tissues. As previously suggested for BR signals perceived in the shoot epidermis (13), ethylene could coregulate cell-autonomous (e.g., mechanical, through shearing at the epidermis/cortex interface) or nonautonomous (e.g., chemical signals or transcription factors) signals moving inward from the epidermis to coordinate growth of the inner tissues. In addition, as growth control by GA was previously mapped to the endodermis (10), balanced root growth probably results from reciprocal communication between the inner and outer layers, with outward signaling from the endodermis. Being adjacent to the vasculature, the latter also allows root-shoot communication and full integration of environmental cues acting above-ground and below-ground.

Materials and Methods

Plant Material and Growth Conditions. *Arabidopsis thaliana* (Col-0) wild-type and *ein2-1* mutant lines were obtained from the Nottingham Arabidopsis Stock Center (NASC; arabidopsis.info/). Ethylene signaling mutant *ctr1-1* was purchased from the Arabidopsis Biological Resource Center, The Ohio State University. The mutant *aux1-22* and *pAUX1::AUX1-YFP* (*aux1-22*) seeds were kindly provided by Malcolm Bennett, The University of Nottingham, Nottingham, UK. The *pEBS::GUS* and *pTAA1::GFP-TAA1* reporters were kindly provided by Anna Stepanova and Jose Alonso, North Carolina State University, Raleigh, NC. R2D2 auxin reporter was received from Dolf Weijers, Wageningen University, Wageningen, The Netherlands. Line *pPIN2::PIN2-GFP* (*pin2*) (39) was obtained from Ben Scheres, Wageningen University, Wageningen, The Netherlands. The *pDR5rev::GFP* and *pGAL4-GFP* enhancer trap lines (M0013, J2104, J0891, J0482, J3611, J2242, J2351, J0301, Q0990, Q2500, J0571, J0951, Q1220, J0121, Q0950, J2104, J2301, J1092, J2341, M0018, Q2393, J0781, J2662, and J1022) (28) were obtained from the NASC. The *pGAL4-GFP* enhancer trap line descriptions are as follows: Jxxxx, prescreened for root expression, Qxxxx, prescreened for root expression; and Mxxxx, prescreened for shoot and floral expression.

The GFP-fusion expression lines (60) (*p35S::GFP*, *pA14::GFP*, *pS2::GFP*, *pS1::GFP*, *pE30::GFP*, *pLRC1::GFP*, and *pQ6::GFP*) were provided by Philip Benfey, Duke University, Durham, NC. The *pML1::GFP* line (61) was obtained from Xuelin Wu, The Salk Institute for Biological Studies, La Jolla, CA.

Molecular Cloning. The promoter sequences used to generate the vectors were previously published (62–67), and the primers used to amplify them are shown in *SI Appendix*, Table S5.

The coding sequences of EBF1 and EBF2 were amplified by RT-PCR with RNA extracted (RNeasy; Qiagen) from untransformed Col-0 plants as a template. Oligonucleotide primers used in the PCR reactions are as follows:

EBF1-forward (F): 5′-AAAAAGCAGGCTCGGTATGTTGGGTATTTGGGGATTAG-3′

EBF1-reverse (R): 5′-AGAAAGCTGGGTGGGCAAAACTAAAGATCTGAGACATG-3′

EBF2-F: 5′-AAAAAGCAGGCTCGCCATGTGTTACGACGTGTAC-3′

EBF2-R: 5′-AGAAAGCTGGGTGGATTCCAGACATAATTCGAAG-3′

*att*B1 EBF1 adapter: 5′-AAAAAGCAGGCTGGATGTCTCAGATCTTTAGTTTTGCC-3′

*att*B2 EBF1 adapter: 5′-AGAAAGCTGGGTGTCAGGAGAGGATGTCACATTT-3′

The PCR products were introduced into pDONR201 (Invitrogen) by recombinational Gateway cloning (Invitrogen). The inserts were fully sequenced to confirm that no PCR or cloning errors had occurred.

The entry clones containing pA14, pS1, pS2 and pE30 promoters were kind gifts from P. Benfey, whereas the destination vectors [pK7WG2 containing the cauliflower mosaic virus (CaMV) 35S promoter, pK7m24GW, pH7m24GW, and pB7WGF2] were from VIB Ghent. The constructs *p35S::EBF1/2*, *pUAS::EBF1*, *pA14::EBF1/2*, *pS1::EBF1/2*, *pS2::EBF1/2*, *pE30::EBF1/2*, *pQ6::EBF1*, *pDR5::EBF2*, *pML1::EBF1/2*, and *pLRC1::EBF2* were generated through MultiSite Gateway Technology (Invitrogen). They were transferred into *Agrobacterium tumefaciens* LBA119 strain. The tissue-specific transactivation lines (*pGAL4-GFP* enhancer trap lines in C24 background) were transformed with *pUAS::EBF1* construct. The other constructs were introduced in wild-type (Col-0) *Arabidopsis* plants.

Lines *pRCH1::GFP-EBF2*, *pCOR::GFP-EBF2*, and *pCo2::GFP-EBF2* (details on vector construction are described in *SI Appendix*, Fig. S9) and the reporter line *pEIN3::genomic EIN3-x3GFP* (*ein3-1*) (*SI Appendix*, Fig. S4) were developed at the Institut de Biologie Moléculaire des Plantes du CNRS, University of Strasbourg. A binary vector pB7WGF2 and BastaRHindIISacICaMV Promoter SpeI eGFP GTW terminator (68) were used for the construction of the vectors *pRCH1::GFP-EBF2*, *pCOR::GFP-EBF2*, and *pCo2::GFP-EBF2*. The EBF2 ORF was PCR-modified with G25T CCCGGGATCCGTATGTCTGGAATCTTCAGAT G25T (BamHI) and G25B GGCTGCAGTTAGTAGAGTATATCGCACCT G25B (stop codon and PstI), cloned to pGem-T Easy (Invitrogen), released by BamHI-NotI digestion, and cloned to BamHI-NotI–digested pENTR1A.

UBI/EBF2 was assembled in pENTR1A (612UbSmaF atcccgggTTGCGTCTGCGTGGAGGTATG and 612UbBamR atggatccccatACCACCACGGAGACGGAGGAC) and cloned to DraIBamHI-digested *pENTR1AEBF2*.

For the construction of the reporter line *pEIN3::genomic EIN3-x3GFP* (*ein3-1*), a genomic fragment of EIN3 upstream regions and ORF minus stop codon was amplified with primers EIN3P F GGTACCAACATATTTGCATCTCTCTATTAGT and EIN3Nco R GGCGCGCCCCATGGCACCAGCGGCGAACCATATGGATACATCTTG, and cloned into a modified pGII-3xGFP vector containing nopaline synthase terminator sequence (tnos). Linker oligonucleotides were inserted into the HindIII and SmaI sites of pGII 3GFP tnos: PacIAscI F agctATTAATTAACCATGGGGCGCGCC (HindIII) and PacIAscI R GGCGCGCCCCATGGTTAATTAAT (SmaI).

The construct was transformed to *ein3-1* mutant.

Ethylene Measurement. The seedlings were grown for 7 days on half-strength Murashige–Skoog medium (1/2 MS) in glass cuvettes for a 16-h/8-h (light/dark) photoperiod. Accumulation of ethylene produced by the seedlings was performed by sealing the cuvettes for 24 h starting on 7th day after germination (DAG). Ethylene was detected with an ETD-300 photoacoustic ethylene detector (Sensor Sense). At least three independent samples (100 seedlings per cuvette) were considered. Ethylene production rate was expressed as picoliters of ethylene produced by a single individual over a period of 24 h.

Ethylene Gas Treatment. Ethylene gas treatments of plants grown on 1/2 MS square plates were performed in specially designed chambers (Van Cleven) comprising a treatment cell and a control cell (1 m^3 each) with identical growth conditions (40% air humidity, temperature of 24 °C, and a 16-h photoperiod). Fresh airflow was installed in the control cell, while the treatment cell was supplemented with a gas mixture (1% ethylene, 20.7% oxygen, and 78.3% nitrogen) under 150-bar pressure. The gas flux was adjusted to maintain constant levels of ethylene of 500 parts per billion (ppb) in the treatment cell. The concentration of ethylene gas in the treatment cell was regularly monitored by analyzing air samples with a selected ion flow tube mass spectrometer.

Phenotypic Analyses. Root elongation assay in a 16-h/8-h photoperiod and scoring of transformant seedlings (at 6 DAG) were performed on vertical plates with 1/2 MS medium containing 1% sucrose and supplemented with 0.5 or 1 μM ACC for plants with a C24 and Col-0 background, respectively. Effects of long-term auxin treatment of transgenic lines in a Col-0 background (*pLRC1::EBF2* and *pA4::EBF2*) were assessed on 6-d-old seedlings grown on 1/2 MS medium containing 1% sucrose and supplemented with 100 nM IAA under a 16-h/8-h photoperiod.

The plates were imaged, and the seedlings were analyzed with RootTrace (69) or/and ImageJ (NIH; https://imagej.nih.gov/ij/) software. At least 20 individuals per line and per treatment were analyzed in each experiment.

Genetic Screen of Ethylene-Insensitive Lines in *aux1-22* Mutant Background. The screen was performed via evaluation of F2 crosses between the recessive *aux1-22* null mutant (with insensitive roots to 1 μM ACC treatment, used as a mother plant) and transgenic lines with cell type-specific EBF2 expression. The respective data in Fig. 6*A* are from at least four independent crossing experiments in which at least 10 F2 individuals with an *aux1* homozygous background were evaluated.

Root Cell Length. For cell length measurements, the seedlings were grown on solid media supplemented with 1 μM ACC. After 6 d, the seedlings (12 per line) were stained with propidium iodide and imaged with a Nikon EZ-C1 confocal microscope. The cell lengths were analyzed on stitched pictures (Fiji software) by using the Cell-o-tape tool (70). The position of each cell was calculated from the cumulative length of all cells lying between the measured cell and the QC. Then, the data were smoothened and interpolated into 25-mm-spaced data points using a linear interpolation function (MS Excel Add-Ins; https://www.microwaves101.com/59-downloads#linterp), allowing the calculation of averages and SDs among replicate roots.

DIC Microscopy and Measurement of Leaf Epidermal Cell Area. Leaves (3, 4) from horizontally grown plants (1/2 MS only or supplemented with 50 μM ACC) were fixed in ethanol/acetic acid (3:1) for 24 h and cleared according to the procedure described by Rodrigues-Pousada et al. (4). The samples were imaged with a dissecting microscope (Axiovert 200M with AxioCamMRm; Zeiss). An area of at least 20 (per genotype and per treatment) neighbor pavement cells from the middle part of the petiole was measured with ImageJ.

Measurement of Fluorescence by Confocal Microscopy. Evaluation of the changes in green intensity (Fig. 6) was done using three independent crosses per line. At least 10 parental reporter and F1 plants were evaluated. The plants from different lines to be compared in confocal observations were usually grown on one and the same plate to omit variations in growth conditions. Subsequently, in each experiment, the observations were made under the same settings of the lasers to allow comparison of fluorescent intensities. The images were taken with a confocal microscope [Nikon EZC1; Plan Apo Lambda (20× objective for crosses with the reporters *pAUX::AUX1-YFP* and *pPIN2::PIN2-GFP*, and 40× objective for crosses with R2D2 sensor)]. Green or/and red florescence intensity was quantified with the Nikon ND2/NIS analysis software and Excel.

Genotyping of T2 Plants with *ctr1-1* Background. The mutant *ctr1-1* background of *pLRC1::EBF2*, *pML1::EBF2*, and *pA14::EBF2* T2 plants was confirmed by genotyping according to the method described by Binder et al. (71). Genotyping was performed by restriction digestion of genomic PCR with MluCI (New England Biolabs) for which the mutation introduces a new restriction site. The genotyping primer sequences are as follows: F primer, ACTCCTCAATTTGTCTTGAAATTTCAGGT; R primer, ACTATTTAGCTTCCATTG-GAAATAGGACC.

Rosette Area Measurements. Plants from the different transgenic lines and the controls (Col-0 and *ein2-1*) were grown horizontally for 14 d on 1/2 MS medium supplemented with 0, 5, 15, or 50 μM ACC (Fig. 4*A* and *SI Appendix*, Fig. S2*B*). Measurements of the rosette area were performed with the Rosette Tracker tool (72) designed to be used with the ImageJ platform. The rosette area and phenotype of *ctr1-1* transgenic lines carrying *pLRC1::EBF2*, *pML1::EBF2*, or *pA14::EBF2* constructs (Fig. 4*C* and *SI Appendix*, Fig. S2*C*) were calculated on day 21 after germination of plants grown on soil (at least 19 individuals from each line were analyzed). Initially the seedlings from the different lines were grown simultaneously for 7 d on 1/2 MS medium to ensure uniform development of the individuals. After that, they were transferred on soil pellets and grown under controlled conditions in growth chamber.

L-Kyn Treatment of Crosses Between Transgenic Lines and *pTAA1::GFP-TAA* Auxin Reporter. Forty-eight-hour dark-grown seedlings were incubated in liquid 1/2 MS medium supplemented with 10 μM ACC, 1.5 μM Kyn, or their combination for an additional 15 h in darkness, followed by confocal observation (with a 20× objective) of the differently treated individuals from each line. F1 crosses between the reporter and Col-0, *pLRC1::EBF2*, and *pA14::EBF2* lines were evaluated. Selected ACC-insensitive F2 individuals from the cross between *pTAA1::GFP-TAA* and *ein2-1* served as ethylene-insensitive controls.

2,4-D Treatment of F1 Crosses Between Transgenic Lines and R2D2 Auxin Reporter. Six-day-old seedlings (F1 crosses between the sensor R2D2, used as a mother plant, and homozygous transgenic lines or Col-0) grown on 1/2 MS medium were treated for 15 min with 50 nM 2,4-D. Changes of fluorescent signal were measured with confocal microscopy (Nikon ND2/NIS analysis software). Calculations were based on measurement of the mDII::ndtTomato/DIIn::x3Venus ratio. At least 20 nuclei of epidermal cells per individual were evaluated, and data were derived from at least three plants per treatment.

Statistical Analysis. All assays were repeated at least three times, with at least 10 (rosette area and fluorescence measurements) or 20 (root length measurement) individuals from each tested line per dataset. Error bars indicate SD. Data were analyzed by two-tailed, unpaired *t* tests (Welch's test) with Holm–Bonferroni sequential correction using Excel software. Asterisks in graphs indicate the level of significance: $*P < 0.05$, $**P < 0.01$, and $***P < 0.001$.

ACKNOWLEDGMENTS. We thank Corina Codreanu for helping with vector constructs and measurements of root cell lengths, Magdalena Baltova and Mathias De Mesmaeker for preliminary experiments regarding cell elongation in root tissues, Justyna Nocon and Bram Van Compernolle for basic cloning steps, and Joke Belza for verifying the ethylene concentration in the ethylene exposure experiment. We also thank Malcolm Bennett for helpful suggestions and critical reading of the manuscript. D.V.D.S. thanks Jiri Friml and Eva Benkova for constructive discussions on auxin-related experiments. D.V.D.S. received financial support from the Research Foundation Flanders (Projects G.0298.09 and G.0656.13N) and Ghent University (BOF-BAS 01B02112). T.P. and P.G. were supported by Laboratoire d'Excellence (Grant ANR-10-LABX-0036_NETRNA).

1. Yang SF, Hoffman NE (1984) Ethylene biosynthesis and its regulation in higher plants. *Annu Rev Plant Physiol* 35:155–189.
2. Kieber JJ (1997) The ethylene signal transduction pathway in Arabidopsis. *J Exp Bot* 48:211–218.
3. Kieber JJ, Rothenberg M, Roman G, Feldmann KA, Ecker JR (1993) CTR1, a negative regulator of the ethylene response pathway in Arabidopsis, encodes a member of the raf family of protein kinases. *Cell* 72:427–441.
4. Rodrigues-Pousada RA, et al. (1993) The Arabidopsis 1-aminocyclopropane-1-carboxylate synthase gene 1 is expressed during early development. *Plant Cell* 5: 897–911.
5. Vandenbussche F, Vaseva I, Vissenberg K, Van Der Straeten D (2012) Ethylene in vegetative development: A tale with a riddle. *New Phytol* 194:895–909.
6. Vanstraelen M, Benková E (2012) Hormonal interactions in the regulation of plant development. *Annu Rev Cell Dev Biol* 28:463–487.
7. Goeschl JD, Rappaport L, Pratt HK (1966) Ethylene as a factor regulating the growth of pea epicotyls subjected to physical stress. *Plant Physiol* 41:877–884.
8. Zhong S, et al. (2014) Ethylene-orchestrated circuitry coordinates a seedling's response to soil cover and etiolated growth. *Proc Natl Acad Sci USA* 111:3913–3920.
9. Ubeda-Tomás S, Beemster GT, Bennett MJ (2012) Hormonal regulation of root growth: Integrating local activities into global behaviour. *Trends Plant Sci* 17:326–331.
10. Ubeda-Tomás S, et al. (2008) Root growth in Arabidopsis requires gibberellin/DELLA signalling in the endodermis. *Nat Cell Biol* 10:625–628.
11. Ubeda-Tomás S, et al. (2009) Gibberellin signaling in the endodermis controls Arabidopsis root meristem size. *Curr Biol* 19:1194–1199.
12. Swarup R, et al. (2005) Root gravitropism requires lateral root cap and epidermal cells for transport and response to a mobile auxin signal. *Nat Cell Biol* 7:1057–1065.
13. Savaldi-Goldstein S, Peto C, Chory J (2007) The epidermis both drives and restricts plant shoot growth. *Nature* 446:199–202.
14. Hacham Y, et al. (2011) Brassinosteroid perception in the epidermis controls root meristem size. *Development* 138:839–848.
15. Dietrich D, et al. (2017) Root hydrotropism is controlled via a cortex-specific growth mechanism. *Nat Plants* 3:17057.
16. Swarup R, et al. (2007) Ethylene upregulates auxin biosynthesis in Arabidopsis seedlings to enhance inhibition of root cell elongation. *Plant Cell* 19:2186–2196.
17. Růzicka K, et al. (2007) Ethylene regulates root growth through effects on auxin biosynthesis and transport-dependent auxin distribution. *Plant Cell* 19:2197–2212.
18. Zhao Q, Guo HW (2011) Paradigms and paradox in the ethylene signaling pathway and interaction network. *Mol Plant* 4:626–634.
19. Chang KN, et al. (2013) Temporal transcriptional response to ethylene gas drives growth hormone cross-regulation in Arabidopsis. *eLife* 2:e00675.
20. Zhang F, et al. (2016) EIN2-dependent regulation of acetylation of histone H3K14 and non-canonical histone H3K23 in ethylene signalling. *Nat Commun* 7:13018.
21. Potuschak T, et al. (2003) EIN3-dependent regulation of plant ethylene hormone signaling by two Arabidopsis F box proteins: EBF1 and EBF2. *Cell* 115:679–689.
22. Guo H, Ecker JR (2003) Plant responses to ethylene gas are mediated by SCF(EBF1/EBF2)-dependent proteolysis of EIN3 transcription factor. *Cell* 115:667–677.
23. Gagne JM, et al. (2004) Arabidopsis EIN3-binding F-box 1 and 2 form ubiquitin-protein ligases that repress ethylene action and promote growth by directing EIN3 degradation. *Proc Natl Acad Sci USA* 101:6803–6808.
24. Li W, et al. (2015) EIN2-directed translational regulation of ethylene signaling in Arabidopsis. *Cell* 163:670–683.
25. Merchante C, et al. (2015) Gene-specific translation regulation mediated by the hormone-signaling molecule EIN2. *Cell* 163:684–697.
26. Barrada A, Montané MH, Robaglia C, Menand B (2015) Spatial regulation of root growth: Placing the plant TOR pathway in a developmental perspective. *Int J Mol Sci* 16:19671–19697.

27. Bleecker AB, Estelle MA, Somerville C, Kende H (1988) Insensitivity to ethylene conferred by a dominant mutation in Arabidopsis thaliana. *Science* 241:1086–1089.
28. Haseloff J (1999) GFP variants for multispectral imaging of living cells. *Methods Cell Biol* 58:139–151.
29. Stepanova AN, Yun J, Likhacheva AV, Alonso JM (2007) Multilevel interactions between ethylene and auxin in Arabidopsis roots. *Plant Cell* 19:2169–2185.
30. Suzuki M, et al. (2015) Transcriptional feedback regulation of YUCCA genes in response to auxin levels in Arabidopsis. *Plant Cell Rep* 34:1343–1352.
31. He W, et al. (2011) A small-molecule screen identifies L-kynurenine as a competitive inhibitor of TAA1/TAR activity in ethylene-directed auxin biosynthesis and root growth in Arabidopsis. *Plant Cell* 23:3944–3960.
32. Stepanova AN, et al. (2008) TAA1-mediated auxin biosynthesis is essential for hormone crosstalk and plant development. *Cell* 133:177–191.
33. Yang ZB, et al. (2014) TAA1-regulated local auxin biosynthesis in the root-apex transition zone mediates the aluminum-induced inhibition of root growth in Arabidopsis. *Plant Cell* 26:2889–2904.
34. Liao CY, et al. (2015) Reporters for sensitive and quantitative measurement of auxin response. *Nat Methods* 12:207–210, 2 p following 210.
35. Teale WD, Paponov IA, Palme K (2006) Auxin in action: Signalling, transport and the control of plant growth and development. *Nat Rev Mol Cell Biol* 7:847–859.
36. Pickett FB, Wilson AK, Estelle M (1990) The aux1 mutation of Arabidopsis confers both auxin and ethylene resistance. *Plant Physiol* 94:1462–1466.
37. Vandenbussche F, et al. (2010) The auxin influx carriers AUX1 and LAX3 are involved in auxin-ethylene interactions during apical hook development in Arabidopsis thaliana seedlings. *Development* 137:597–606.
38. Swarup R, et al. (2004) Structure-function analysis of the presumptive Arabidopsis auxin permease AUX1. *Plant Cell* 16:3069–3083.
39. Jones AR, et al. (2009) Auxin transport through non-hair cells sustains root-hair development. *Nat Cell Biol* 11:78–84.
40. Xu J, Scheres B (2005) Dissection of Arabidopsis ADP-RIBOSYLATION FACTOR 1 function in epidermal cell polarity. *Plant Cell* 17:525–536.
41. Barlow PW (2002) The root cap: Cell dynamics, cell differentiation and cap function. *J Plant Growth Regul* 21:261–286.
42. Baluška F, Mancuso S (2013) Root apex transition zone as oscillatory zone. *Front Plant Sci* 4:354.
43. Dello Ioio R, et al. (2008) A genetic framework for the control of cell division and differentiation in the root meristem. *Science* 322:1380–1384.
44. Gaillochet C, Lohmann JU (2015) The never-ending story: From pluripotency to plant developmental plasticity. *Development* 142:2237–2249.
45. Dugardeyn J, Vandenbussche F, Van Der Straeten D (2008) To grow or not to grow: What can we learn on ethylene-gibberellin cross-talk by in silico gene expression analysis? *J Exp Bot* 59:1–16.
46. Muday GK, Rahman A, Binder BM (2012) Auxin and ethylene: Collaborators or competitors? *Trends Plant Sci* 17:181–195.
47. Street IH, et al. (2015) Ethylene inhibits cell proliferation of the Arabidopsis root meristem. *Plant Physiol* 169:338–350.
48. Pacheco-Villalobos D, et al. (2016) The effects of high steady state auxin levels on root cell elongation in Brachypodium. *Plant Cell* 28:1009–1024.
49. Mano Y, Nemoto K (2012) The pathway of auxin biosynthesis in plants. *J Exp Bot* 63: 2853–2872.
50. Pacheco-Villalobos D, Sankar M, Ljung K, Hardtke CS (2013) Disturbed local auxin homeostasis enhances cellular anisotropy and reveals alternative wiring of auxin-ethylene crosstalk in Brachypodium distachyon seminal roots. *PLoS Genet* 9:e1003564.
51. Barbez E, Dünser K, Gaidora A, Lendl T, Busch W (2017) Auxin steers root cell expansion via apoplastic pH regulation in *Arabidopsis thaliana*. *Proc Natl Acad Sci USA* 114:E4884–E4893.
52. Chadwick AV, Burg SP (1970) Regulation of root growth by auxin-ethylene interaction. *Plant Physiol* 45:192–200.
53. Evans ML, Ishikawa H, Estelle MA (1994) Responses of Arabidopsis roots to auxin studied with high temporal resolution: Comparison of wild type and auxin-response mutants. *Planta* 194:215–222.
54. Müssig C, Shin GH, Altmann T (2003) Brassinosteroids promote root growth in Arabidopsis. *Plant Physiol* 133:1261–1271.
55. Fu X, Harberd NP (2003) Auxin promotes Arabidopsis root growth by modulating gibberellin response. *Nature* 421:740–743.
56. Yu H, et al. (2013) ROOT ULTRAVIOLET B-SENSITIVE1/weak auxin response3 is essential for polar auxin transport in Arabidopsis. *Plant Physiol* 162:965–976.
57. Staal M, et al. (2011) Apoplastic alkalinization is instrumental for the inhibition of cell elongation in the Arabidopsis root by the ethylene precursor 1-aminocyclopropane-1-carboxylic acid. *Plant Physiol* 155:2049–2055.
58. Mulkey TJ, Kuzmanoff KM, Evans ML (1982) Promotion of growth and hydrogen ion efflux by auxin in roots of maize pretreated with ethylene biosynthesis inhibitors. *Plant Physiol* 70:186–188.
59. Dyson RJ, et al. (2014) Mechanical modelling quantifies the functional importance of outer tissue layers during root elongation and bending. *New Phytol* 202:1212–1222.
60. Lee JY, et al. (2006) Transcriptional and posttranscriptional regulation of transcription factor expression in Arabidopsis roots. *Proc Natl Acad Sci USA* 103:6055–6060.
61. Wu X, et al. (2003) Modes of intercellular transcription factor movement in the Arabidopsis apex. *Development* 130:3735–3745.
62. Brady SM, et al. (2007) A high-resolution root spatiotemporal map reveals dominant expression patterns. *Science* 318:801–806.
63. Sessions A, Weigel D, Yanofsky MF (1999) The Arabidopsis thaliana MERISTEM LAYER 1 promoter specifies epidermal expression in meristems and young primordia. *Plant J* 20:259–263.
64. Casamitjana-Martínez E, et al. (2003) Root-specific CLE19 overexpression and the sol1/2 suppressors implicate a CLV-like pathway in the control of Arabidopsis root meristem maintenance. *Curr Biol* 13:1435–1441.
65. Dinneny JR, et al. (2008) Cell identity mediates the response of Arabidopsis roots to abiotic stress. *Science* 320:942–945.
66. Heidstra R, Welch D, Scheres B (2004) Mosaic analyses using marked activation and deletion clones dissect Arabidopsis SCARECROW action in asymmetric cell division. *Genes Dev* 18:1964–1969.
67. Karimi M, Inzé D, Depicker A (2002) GATEWAY vectors for Agrobacterium-mediated plant transformation. *Trends Plant Sci* 7:193–195.
68. Walker JM, Vierstra RD (2007) A ubiquitin-based vector for the co-ordinated synthesis of multiple proteins in plants. *Plant Biotechnol J* 5:413–421.
69. French A, Ubeda-Tomás S, Holman TJ, Bennett MJ, Pridmore T (2009) High-throughput quantification of root growth using a novel image-analysis tool. *Plant Physiol* 150:1784–1795.
70. French AP, et al. (2012) Identifying biological landmarks using a novel cell measuring image analysis tool: Cell-o-Tape. *Plant Methods* 8:7.
71. Binder BM, et al. (2007) The Arabidopsis EIN3 binding F-box proteins EBF1 and EBF2 have distinct but overlapping roles in ethylene signaling. *Plant Cell* 19:509–523.
72. De Vylder J, Vandenbussche F, Hu Y, Philips W, Van Der Straeten D (2012) Rosette tracker: An open source image analysis tool for automatic quantification of genotype effects. *Plant Physiol* 160:1149–1159.